Wharton's Jelly Derived Mesenchymal Stem Cells: Comparing Human and Horse

Wharton's jelly derived mesenchymal stem cells: comparing human and horse

Barbara Merlo[a*] , Gabriella Teti[b], Eleonora Mazzotti[b], Laura Ingrà[b], Viviana Salvatore[b],

Marina Buzzi[c], Giorgia Cerqueni[d], Manuela Dicarlo[d], Aliai Lanci[a], Carolina Castagnetti[a], Eleonora Iacono[a]

[a]Department of Veterinary Medical Sciences, University of Bologna, via Tolara di Sopra 50, 40064 Ozzano Emilia (BO), Italy

[b]Department for Biomedical and Neuromotor Sciences, University of Bologna, via Irnerio 48, 40126 Bologna (BO), Italy

[c]Banca dei Tessuti, del Sangue cordonale e Biobanca Policlinico S.Orsola-Malpighi, Bologna, Italy

[d]Department of Clinical and Molecular Sciences, Polytechnic University of Marche, Ancona, Italy

*Corresponding author: Prof. Barbara Merlo, via Tolara di Sopra 50, 40064 Ozzano Emilia (BO), Italy; barbara.merlo@unibo.it

Conflict of Interest

The authors declare that they have no conflict of interest.

Summary

Wharton's jelly (WJ) is an important source of mesenchymal stem cells (MSCs) both in human and other animals. The aim of this study was to compare human and equine WJMSCs. Human and equine WJMSCs were isolated and cultured using the same protocols and culture media. Cells were characterized by analysing morphology, growth rate, migration and adhesion capability, immunophenotype, differentiation potential and ultrastructure. Results showed that human and equine WJMSCs have similar ultrastructural details connected with intense synthetic and metabolic activity, but differ in growth, migration, adhesion capability and differentiation potential. In fact, at the scratch assay and transwell migration assay, the migration ability of human WJMSCs was higher ($P<0.05$) than that of equine cells, while the volume of spheroids obtained after 48 h of culture in hanging drop was larger than the volume of equine ones ($P<0.05$), demonstrating a lower cell adhesion ability. This can also revealed in the lower doubling time of equine cells (3.5±2.4 days) as compared to human (6.5±4.3 days) ($P<0.05$), and subsequently in the higher number of cell doubling after 44 days of culture observed for the equine (20.3±1.7) as compared to human cells (8.7±2.4) ($P<0.05$), and to the higher ($P<0.05$) ability to form fibroblast colonies at P3. Even if in both species tri-lineage differentiation was achieved, equine cells showed an higher chondrogenic and osteogenic differentiation ability ($P<0.05$). Our findings indicate that, although the ultrastructure demonstrated a staminal phenotype in human and equine WJMSCs, they showed different properties reflecting the different sources of MSCs.

Keywords: mesenchymal stem cell, Wharton's jelly, horse, human, transmission electron microscopy

Introduction

Mesenchymal stem cells (MSCs) are defined as a population of multipotent stem cells capable of plastic-adherence when maintained in standard culture conditions, expression typical mesenchymal surface molecules (CD105, CD73 and CD90) and lacking hematopoietic ones (CD45, CD34, CD14 or CD11b, CD79α or CD19 and HLA-DR), and able to differentiate into osteoblasts, adipocytes and chondroblasts in vitro (1). Since these properties, MSCs offer a great chance for cell-based therapies and tissue engineering applications.

Placental tissues and foetal fluids represent a source of cells for regenerative medicine. They are readily available and easily procured without invasive procedures. MSCs from foetal fluids and adnexa are defined as an intermediate between embryonic and adult stem cells, due to the preservation of some characteristics typical of the primitive native layers.

Umbilical cord is routinely discarded at parturition and its extracorporeal nature facilitates isolation by eliminating the invasive and discomfort extraction procedures as well as patient risks that attend adult stem cell isolation. Most significantly, the comparatively large volume of umbilical cord and ease of physical manipulation theoretically increase the number of stem cells that can be extracted, which make it possible to get substantial number of cells in several passages without need of long term culture and extensive expansion ex vivo. Both in human and animals, multipotent stem cells are isolated from the mesenchyme-like cushioning material called "Wharton's jelly" (WJ) found between the vessels of the umbilical cord (2,3). WJ cells represent an unique, easily accessible, and non-controversial source of early stem cells that can be readily manipulated. MSCs derived from Wharton's jelly (WJMSCs) are easier to isolate and expand than MSCs from other fetal and adult tissues, and impact fields such as regenerative medicine, biotechnology and agriculture (4).

The field of regenerative medicine is approaching translation to clinical practice, and significant safety concerns and knowledge gaps have become clear as clinical practitioners are considering the potential risks and benefits of cell-based therapy. It is necessary to understand the full spectrum of stem cell actions and preclinical evidence for safety and therapeutic efficacy. The role of animal models for gaining this information has increased substantially. There is an urgent need for novel animal models to expand the range of current studies, most of which have been conducted in rodents. Extant models are providing important information but have limitations for a variety of disease categories and can have different size and physiology relative to humans (5). Before human clinical trials are undertaken, stem cell-based therapies for non-life threatening disorders should be evaluated for their safety and efficacy using animal models of spontaneous disease and not solely by the existing laboratory models of experimentally induced lesions. The horse lends itself as a good animal model of different spontaneous disorders that are clinically relevant to similar human disorders. The development of large animal experimental models, including horse, may open alternative strategies for investigating placental MSCs physiology and potential application for human and veterinary regenerative medicine. The objective of

this study was to compare human and equine WJMSCSs obtained following the same protocols in order to define similarities and differences, also at ultrastructural level, that can be useful in understanding species-specific characteristics and in defining new animal models.

Materials and Methods

Chemicals were obtained from Sigma Aldrich (St. Louis, MO, USA) and laboratory plastic ware was from Sarstedt Inc. (Newton, NC, USA) and Corning (Corning, NY, USA), unless otherwise stated.

Human and equine cells isolation and expansion

hWJMSCs and eWJMSCs were obtained from tissue of umbilical cords of respectively 7 and 10 full-term pregnancies. Informed consent was obtained from each patient according to the guidelines of the National Bioethics Committee and the samples were treated following a protocol approved by the University of Bologna. For equine samples, the written consent was given by the owners to allow tissues recovery for research purposes.

Wharton's jelly was cut in small fragments and digested with collagenase (Gibco, Thermo Fisher, Monza, Italy) 0.1% (w/v) in phosphate buffer saline (PBS) at 37°C approximately for 3 hours. Then, samples were washed in PBS with 10% (v/v) fetal bovine serum (FBS) (Gibco, Thermo Fisher, Monza, Italy) several times, centrifuged at 400g for 50 minutes and finally re-suspended in DMEM/F12 Glutamax® medium (Gibco, Thermo Fisher, Monza, Italy) supplemented with 10% FBS (v/v), 1% (v/v) penicillin and streptomycin (Gibco, Thermo Fisher, Monza, Italy). Primary cells were plated in a 25 cm^2 flask, as "Passage 0" (P0), at a density of $5x10^3$ cell/cm^2 and incubated in 5% (v/v) CO_2 humidified atmosphere at 37°C (human) or 38.5°C (equine). The medium was completely replaced every 3 days until the adherent cell population reached about 80% confluence. At this point, the adherent primary MSCs were passaged by digestion with 0.25% (w/v) trypsin-EDTA, counted with a haemocytometer, and reseeded as P1 at $5x10^3$ cells/cm^2. For the subsequent passages (P1-P6), cells were inoculated in 25 cm^2 flasks at $5x10^3$ cells/cm^2 and allowed to multiply to 90% confluence before trypsinization and successive passage. Cell-doubling time (DT) and cell-doubling numbers (CD) and cell culture time (CT) were calculated from haemocytometer counts for each passage according to the following two formulae (6):

$$CD=\ln(Nf/Ni)/\ln(2)$$

$$DT=CT/CD$$

where Nf and Ni are the final and initial number of cells, respectively.

Cells at P3 were used for the subsequent determination and characterization.

CFU-F assay

To assess CFU-F, 100 cells from each population were seeded at P3 in 35 mm petri dish and cultured for 12 days. Colonies were fixed in methanol and stained with Giemsa. Colonies formed by at least 16–20 nucleate cells were counted using an inverted light microscope (Eclipse TE 2000u, Nikon Instruments Spa, Florence, Italy).

Scratch assay

Cells ($4.8x10^4$) were seeded on 35 mm petri dishes and cultured until confluence in the same conditions as previously described. Scratches were made using 1 mL pipette tips, washed with medium and allowed to grow for additional 24 h. Immediately after the scratch and at the end of the culture, cells were observed under an inverted light microscope (Motic AE21, VWR International Srl, Milan, Italy; Eclipse TE 2000u, Nikon Instruments Spa, Florence, Italy) and photographed in the same area (marked in the plate) by CCD camera (Visicam 3.0, VWR International Srl, Milan, Italy; DS-Fi2, Nikon Instruments Spa, Florence, Italy). Gap distance of the wound was measured using Image J software (Version 1.48s; National Institutes of Health, USA). The migration percentages were calculated using the following formula:

[(distance at time 0–distance at 24 h)*100]/distance at time 0

Transwell migration assay

MSCs migratory ability was assessed by a 24-well transwell system inserting a 8 μm pore size filter membrane (Millipore, Milan, Italy). $1x10^4$ cells in a serum-free medium of 100 μL volume were added to the upper chamber, and 600 μL medium containing 10% FBS was added to the bottom chamber and cultured in the same conditions as previously described. After 22 h incubation, the cells on the upper surface of the filter membrane were removed, whereas the migrated cells on the undersurface of the filter membrane were fixed with methanol and stained with Diff-Quik (Bio-Optica, Milan, Italy). Cells migrated to the lower surface of the filter were imaged (DS-Fi2, Nikon Instruments Spa, Florence, Italy) using an inverted light microscope (Eclipse TE 2000u, Nikon Instruments Spa, Florence, Italy) and counted. Ten fields from each filter were randomly chosen to determine the number of migrated cells.

Adhesion test (hanging drop culture)

25 μl drops of cell medium, containing approximately $5x10^3$ cells each, were pipetted on the inner side of the lid of a 90 mm petri dish, which was gently inverted and allowed to grow for 48 h in the same cell culture conditions as previously described. Then, cells were observed under an inverted light microscope (Motic AE21, VWR International Srl, Milan, Italy; Eclipse TE 2000u, Nikon Instruments Spa, Florence, Italy) and photographed by CCD camera (Visicam 3.0, VWR International Srl, Milan, Italy; DS-Fi2, Nikon Instruments Spa, Florence, Italy). Area and volume of cell masses obtained were obtained by using Image J software and ReVisp software (7).

Immunophenotyping by flow cytometry

The cells obtained were checked for their mesenchymal profile by FACSCalibur flow cytometry system (Becton Dickinson, CA, USA). 2.5×10^5 cells were distributed to 5 ml round-bottom polystyrene tubes, washed with Dulbecco PBS and were then stained for 45 min with the following antibodies: fluorescein isothiocyanate-(FITC)-labeled mouse anti-human CD90 (StemCell Technologies, Milan, Italy), CD105, CD14, CD19 and CD34 (Immunotools, Germany), R-phycoerythrin -(PE)-labeled mouse anti-human CD45 (Diaclone, France), CD73 (Becton Dickinson, CA, USA), and HLA-DR (Diaclone, France). The control for FITC- or PE-coupled antibodies was isotypic mouse IgG1. The data were analysed using FCS Express 6 Plus Software (De Novo Software, CA, USA).

Transmission Electron Microscopy (TEM)

WJMSCs, cultured in monolayers, were fixed with 2.5% (v/v) glutaraldehyde in 0.1 mol/l cacodylate buffer for 2 h and post fixed with a solution of 1% (w/v) osmium tetroxide in 0.1 mol/l cacodylate buffer. The cells were then embedded in epoxy resins after a graded-ethanol serial dehydration step. The embedded cells were sectioned into ultrathin slices, stained by uranyl acetate solution and lead citrate, and then observed with transmission electron microscope CM10 Philips (FEI Company, Eindhoven, The Netherlands) at an accelerating voltage of 80 kV. Images were recorded by Megaview III digital camera (FEI Company, Eindhoven, The Netherlands). TEM analysis were performed in duplicate for cells obtained from each human and equine sample. Cellular details were calculated on 20 different fields for each sample, acquired at 19000X magnification by Megaview software system (FEI Company, Eindhoven, The Netherlands).

Differentiation

WJMSCs were seeded in six-well culture plates at a density of $1.25\text{x}10^4$ in the same culture condition as previously described. After 24 h, medium was completely replaced with adipogenic, chondrogenic and ostegenic induction medium. Adipogenic medium: DMEM/F12 + 15% (v/v) rabbit serum + 1 µmol/l dexamethasone (removed after 6 days) +0.5 mmol/l IBMX (3-isobutyl-1-methylxanthine) (removed after 3 days), 10 µg/ml insulin, 0.2 mmol/l indomethacin. Chondrogenic medium: DMEM/F12 + 1% (v/v) FBS + 6.25 µg/ml insulin + 50 nM AA2P (2-phospho-L-ascorbic acid trisodium salt), 0.1 µmol/l dexamethasone, 10 ng/ml hTGFβ1 (human transforming growth factor β1). Osteogenic medium: DMEM/F12 + 10% (v/v) FBS + 10 mmol/l beta-glycerophosphate + 0.1 µmol/l dexamethasone + 50 µmol/l AA2P.

To assess differentiation, cells were fixed with 10% (w/v) formalin for 1 h, and then stained. Oil Red O (0.3% (v/v) in 60% (v/v) isopropanol) was used to evaluate formation of neutral lipid vacuoles after 10 days of adipogenic

differentiation. Chondrogenic and osteogenic differentiation were assessed after 21 days of culture in induction media by using 1% (w/v) Alcian Blue in 3% (v/v) acetic acid solution and 2% (w/v) Alizarin Red S (pH 4.1–4.3) solution, respectively. Cells were observed under an inverted light microscope (Motic AE21, VWR International Srl, Milan, Italy; Eclipse TE 2000u, Nikon Instruments Spa, Florence, Italy) and photographed by CCD camera (Visicam 3.0, VWR International Srl, Milan, Italy; DS-Fi2, Nikon Instruments Spa, Florence, Italy). Control samples consisted in WJMSCs cultured for the same period of time in DMEM/F12 plus 2% (v/v) FBS.

Images obtained after differentiation were analysed for colour intensity using Image J software (National Institutes of Health, USA) in order to compare the differentiation ability of human and equine WJMSCs.

Statistical analysis

Growth curves were obtained from 3 samples per species. Tests and analysis were performed on P3 cells. Scratch and adhesion assays were done on 2 samples for each species, collecting data from 5 replicates per sample. CFU-F and transwell migration assays were done on 3 samples per species and 3 replicates per sample. FACS analysis, TEM and differentiation were performed on 3 samples for each species. Data are expressed as mean ± SD. Data were analysed for normality using a Shapiro-Wilk test. Statistical differences were assessed by Student t Test or Mann-Whitney U test and by Friedman test using the software IBM SPSS Statistics 23 (IBM Corporation, Milan, Italy). Significance was assessed for $P<0.05$.

Results

Primary culture of WJMSCs

Both human and equine cells obtained from each umbilical cord, were adherent cells showing a fibroblast like morphology. Cells were cultured up to P6 and mean DT was higher ($P<0.05$) for human (6.5±4.3 days) than equine (3.5±2.4 days) cells. No significant differences ($P>0.05$) between all passages were observed for human cells while eWJMSCs showed a trend to DT increasing starting from P4 ($P<0.05$) (Fig. 1). Total cell doublings after 44 days of culture were higher ($P<0.05$) in the horse (20.3±1.7) as compared to hWJMSCs (8.7±2.4).

CFU-F assay

The mean number of fibroblast colonies for 100 P3 eWJMSCs plated was 53.5 ± 18.4 (range 40-79), while CFU-F could not be demonstrated in hWJMSCs after 12 days of culture.

Scratch assay

In order to evaluate the ability of WJSCMs to migrate, a scratch assay was performed. Results showed, in both species, a good capacity of cells to proliferate and partially cover the cell free area after 24 h of culture, but hWJMSC reached a higher ($P<0.05$) migration rate (58.5±4.7%) as compared to eWJMSCs (43.0±7.7%).

Transwell migration assay

In order to quantify the ability of MSCs to migrate in presence of a chemoattractant (FBS), transwell migration assay was performed. A higher migration ability ($P<0.05$) for hWJMSCs (15.2±13.5) was found as compared to equine cells (3.5±2.3).

Adhesion assay

In order to evaluate the ability of WJMSCs to adhere each other, the adhesion assay was carried out. Results showed a higher ability for eWJMSCs than hWJMSCs to aggregate each other, as demonstrated by the lower ($P<0.05$) mean volume of the equine spheroids compared to human ones (Fig. 2A). Furthermore, the lower adhesion ability of hWJMSC was also observed since more frequently (about 50%) generating micro-masses (Fig. 2B).

Immunophenotyping of WJMSCs by flow cytometry

In order to evaluate the mesenchymal phenotype, both human and equine WJMSCs obtained were characterize by flow cytometry. According to Dominici et al. (2006), the expression of the following markers was evaluated: CD105, CD73, CD90, CD14, CD19, CD34, CD45 and HLA-DR. hWJMSCs were highly positive for CD105, CD73 and CD90 and negative for CD34, CD19, CD45, CD14 and HLA-DR (Tab. 1 and Fig. 3). Using a pre-set antibody panel for human cells, most of the clones used were not suitable for equine cells, since cross-reactivity was lacking, as previously demonstrated (8-10). As consequence, eWJMSCs were evaluated only for the expression of CD90 (Tab. 1 and Fig. 3). Furthermore, no cross-reactivity CD19 (clone LT-19) was demonstrated, as it was not able to bind equine lymphocytes (positive control, data not shown).

TEM analysis

TEM analysis was performed to evaluate ultrastructure of cells with the final goal to establish morphological parameters useful for the classification and comparison of human and equine WJMSCs.

hWJMSCs are spindle like shape cells with an average area of 600 μm^2, characterized by large euchromatic nucleus and one nucleolus each (Fig. 4A). At middle magnification, a widely developed Golgi apparatus (Fig. 4B) surrounded by several secretory vesicles with a diameter ranging from 70 to 200 nm, rough endoplasmic reticulum (RER) with cisternae

showing moderately electron dense material and mitochondria with evident internal cristae were observed (Fig. 4C). An high number of free ribosomes, randomly distributed, characterized the cytoplasm. Several autophagic vesicles and autophagolysosomes with an average diameter of 600 nm, were observed in the cytoplasm of hWJMSCs (Fig. 4D). Cellular junctions were observed between cells grown in monolayer after reaching the confluence (Fig. 4D insert).

EWJMSCs appear as large fibroblastic like cells, with an average diameter of 700 μm^2, showing euchromatic nucleus and a variable number of nucleolus ranging from 2 to 6 each cell (Fig. 4E). At higher magnification, Golgi apparatus, often in more than one each cell, surrounded by several small vesicles with a diameter ranging from 50 to 250 nm, widespread in the cytoplasm (Fig. 4F). RER cisternae were numerous and partially enlarged, showing a moderately electron dense material. An high number of elongate mitochondria with evident internal cristae were also observed (Fig. 4G). Autophagy vesicles and autophagolysosomes, with an average number of 18 each field, and diameter ranging from 450 nm to 700 nm, characterized the cytoplasm (Fig. 4H). An high number of free ribosomes and a few lipid droplets were randomly observed in the cytoplasm. Cell junctions were observed (Fig. 4H insert).

Differentiation

Oil Red O showed the presence of several fat droplets in almost all cells after 10 days of differentiation both in human (Fig. 5A) and equine (Fig. 6A) cells, compared to control samples in which no fat droplets were detected (Fig. 5B, Fig. 6B). Furthermore, a change in cell morphology is clearly apparent for both human and equine lineages.

Also for chondrogenic differentiation, control samples stained negative for Alcian Blue (Fig. 5D; Fig. 6D). while a strong blue colour in cells and extracellular matrix after 21 days of differentiation in both species (Fig. 5C human; Fig. 6C equine) suggested a gradual deposition of glycosaminoglycans.

A strong red colour in cells and extracellular matrix after 21 days of osteogenic differentiation in human (Fig. 5E) and equine (Fig. 6E) cells confirmed the deposition of calcium, and the presence of mineralized extracellular matrix, which was undetectable by alizarin red in control samples (Fig. 5F; Fig. 6F).

No differences ($P>0.05$) in the level of adipogenic differentiation were observed between human and equine WJMSCs, while eWJMSCs showed an higher ($P<0.05$) chondrogenic and osteogenic differentiation potential as compared to human counterparts, as demonstrated by the lower mean grey value observed after colour intensity analysis of differentiation images.

Discussion

In this study, MSCs were successfully isolated from equine and human Wharton's jelly by tissue digestion using the same protocol. Further analysis of proliferation, migration, adhesion, immunophenotyping, tri-lineage differentiation and TEM

behaviour of isolated MSCs was performed for comparative evaluation of WJMSCs from both species. TEM analysis confirmed the presence of an intense metabolism and secretory activity, all morphological features linked with the maintenance of cell stemness and survival. Interestingly, major differences between cellular properties of hWJMSCs and eWJMSCs were observed in the proliferation, migration, adhesion abilities and also in differentiation potential.

For this study, the horse was chosen as an appropriate animal model, since there are pathophysiological similarities between human and equine orthopaedic diseases (11). Furthermore, in equine medicine the treatment of orthopaedic injuries with MSCs is currently widely used (12-14). Wharton's jelly is a plentiful and inexpensive source of cells that fit into the category of primitive stromal cells (4), so in the present study it was chosen as donor tissue.

In both species, TEM analysis showed cells with a fibroblast shape, large nucleus, well developed RER and Golgi apparatus surrounded by several mitochondria, ultrastructural characteristics connected with a proliferating status and an intense synthetic and metabolic activity, which characterize mesenchymal stem cells (15). Equine WJMSCs showed a higher number of nucleoli, ranging from 2 to 6, comparing to the human WJMSCs, in which one nucleolus was always detected. The number of nucleolus is correlated with an intense protein synthesis and metabolic activity due to an increased demand for proteins during cell growth and proliferation which reflects an increase in protein synthetic capacity by upregulating ribosome biogenesis (16). The higher number of nucleolus in eWJMSCs is in agreement with our findings on cellular properties of eWJMSCs and hWJMSCs in which eWJMSCs demonstrated a higher proliferation, adhesion abilities and differentiation potential compared to hWJMSCs.

Furthermore, in both species a large amount of vesicles was observed in the cytoplasm, as previously reported in equine adipose derived mesenchymal stem cells where an high amount of primary endocytic vesicles, early endosomes, late endosomes, endolysosomes and lysosomes (eAdMSCs) (17). In human mesenchymal stem cells, it was also reported the presence of autophagic vacuoles inside amnion MSCs (15,18), in agreement with our observations in which an high number of autophagy vesicles and autophagosomes were detected. Recently, it has been demonstrated the presence of a constitutive autophagy as a cytoprotective and cellular quality control mechanisms to balance protein and organelle turnover, crucial for the maintenance of stemness (19,20).

The first observation arose from proliferation assay is that equine WJMSCs grew more rapidly in comparison to human cells. Also the ability to form fibroblast colonies at P3 in 12 days confirmed that observation. Mean doubling time for equine cells was lower, but while human cells did not exhibit variation in the first 6 passages, an increase was observed by P4 for eWJMSCs. The quite early increasing of DT of eWJMSCS observed in this study has never been observed before in our laboratory, and subsequently mean doubling time was higher than in previous studies (21). A possible explanation could be that, for the present research, the culture medium was changed, and equine cells were cultured in

the same medium routinely used for human MSCs (22). Further studies culturing eWJMSCs in different conditions are needed to ascertain such hypothesis.

Migration potential of MSCs is considered important for their integration into the host tissue during therapeutic applications (23). In the present study, hWJMSCs showed a trend towards increased migration activity in comparison to eWJMSCs, suggesting their graft integration in vivo may be enhanced. This finding was surprising, given that human cells showed a slower doubling time, but could be partially explained by the observed lower cell-to-cell adhesion potential. In fact, hWJMSCs spheroids after hanging drop culture were larger than those formed by eWJMSCs, and quite often fragmented, demonstrating a lower self-assembly ability. Self-assembly of MSCs into aggregates has significant implication in their applications in cell therapy and tissue regeneration (24). 3D spheroid culture system contributes to an optimization for efficient in vitro differentiation of MSCs (25) and in vivo MSC 3D transplantation of synovial MSC aggregates promoted cartilage tissue regeneration in a rabbit model (26).

In this study, no significant differences were observed in the adipogenic differentiation capacity between hWJMSCs and eWJMSCs, on the contrary, eWJMSCs produced more extracellular matrix both in chondrogenic and osteogenic differentiation, as confirmed by an higher intensity of staining. Differentiations were performed using standard protocols described in the literature for human MSCs (27), with some modifications (21): for the chondrogenic differentiation 0.1 mM dexamethasone was added, while rabbit serum was used for the adipogenic differentiation protocol. Indeed, it has been reported that rabbit serum enhances adipogenic differentiation (28).

Analysis of surface marker expression patterns provided further insights into the characteristics of human MSCs, but only one antibody of the panel available was cross-reacting with equine epitopes. This study confirms what already observed by others in the horse (9,10,29), and adds to the list a new antibody that does not recognize the corresponding equine epitope (CD 19, clone LT-19).

In conclusion, our findings indicate that MSCs isolated from umbilical cord of different species have a similar ultrastructure compatible with mesenchymal stem phenotype, which makes them to have different biological proprieties. Nevertheless, human and equine WJMSCs differ in growth, migration, adhesion capability and differentiation potential. This study helps to better clarify the specie-specific characteristics and in defining new animal models.

Acknowledgements

The author wish to thank Mirella Falconi, manager of “Laboratorio di morfologia e biologia cellulare e tissutale” (Department for Biomedical and Neuromotor Sciences). This research was funded by RFO (Ricerca Fondamentale Orientata), University of Bologna.

References

1. Dominici, M., Le Blanc, K., Mueller, I., et al. (2006). Minimal criteria for defining multipotent mesenchymal stromal cells. The International Society for Cellular Therapy position statement. Cytotherapy, 8, 315-317.

2. Vangsness, C.T. Jr., Sternberg, H., Harris, L. (2015). Umbilical cord tissue offers the greatest number of harvestable mesenchymal stem cells for research and clinical application: a literature review of different harvest sites. Arthroscopy, 31, 1836-1843.

3. Iacono, E., Rossi, B., Merlo, B. (2015). Stem cells from foetal adnexa and fluid in domestic animals: an update on their features and clinical application. Reprod Domest Anim, 50, 353-364.

4. Troyer, D.L., Weiss, M.L. (2008). Wharton's jelly-derived cells are a primitive stromal cell population. Stem Cells, 26, 591-599.

5. Harding, J., Roberts, R.M., Mirochnitchenko, O. (2013). Large animal models for stem cell therapy. Stem Cell Research & Therapy, 4, 23.

6. Rainaldi, G., Pinto, B., Piras, A., Vatteroni, L., Simi, S., Citti, L. (1991). Reduction of proliferative heterogeneity of CHEF18 Chinese hamster cell line during the progression toward tumorigenicity. In Vitro Cell Dev Biol, 27, 949-952.

7. Piccinini, F., Tesei, A., Arienti, C., Bevilacqua, A. (2015). Cancer multicellular spheroids: volume assessment from a single 2D projection. Comput Methods Programs Biomed, 118, 95-106.

8. De Schauwer, C., Piepers, S., Van de Walle, G.R., et al. (2012). In search for cross-reactivity to immunophenotype equine mesenchymal stromal cells by multicolor flow cytometry. Cytometry A, 81, 312-323.

9. Ibrahim, S., Steinbach, F. (2012). Immunoprecipitation of equine CD molecules using anti-human MABs previously analyzed by flow cytometry and immunohistochemistry. Vet Immunol Immunopatholo, 145, 7-13.

10. Iacono, E., Merlo, B., Romagnoli, N., Rossi, B., Ricci, F., Spadari, A. (2015). Equine bone marrow and adipose tissue mesenchymal stem cells: cytofluorimetric characterization, in vitro differentiation, and clinical application. J Eq Vet Sci, 35, 130-140.

11. Patterson-Kane, J.C., Becker, D.L., Rich, T. (2012). The pathogenesis of tendon microdamage in athletes: the horse as a natural model for basic cellular research. J Comp Pathol, 147, 227-247.

12. Smith, R.K.W. (2008). Mesenchymal stem cell therapy for equine tendinopathy. Disabil Rehabil, 30, 1752-1758.

13. Crovace, A., Lacitignola, L., Rossi, G., Francioso, E. (2010). Histological and immunohistochemical evaluation of autologous cultured bone marrow mesenchymal stem cells and bone marrow mononucleated cells in collagenase-induced tendinitis of equine superficial digital flexor tendon. Vet Med Int, 250978.

14. Godwin, E.E., Young, N.J., Dudhia, J., Beamish, I.C., Smith, R.K. (2012). Implantation of bone marrow-derived mesenchymal stem cells demonstrates improved outcome in horses with overstrain injury of the superficial digital flexor tendon. Equine Vet J, 44, 25-32.

15. Pasquinelli, G., Tazzari, P., Ricci, F., et al. (2007). Ultrastructural characteristics of human mesenchymal stromal (stem) cells derived from bone marrow and term placenta. Ultrastruct Pathol, 31, 23-31.

16. Orsolic, I., Jurada, D., Pullen, N., Oren, M., Eliopoulos, A.G., Volarevic, S. (2016). The relationship between the nucleolus and cancer: Current evidence and emerging paradigms. Semin Cancer Biol, 37-38, 36-50.

17. Pascucci, L., Mercati, F., Marini, C., et al. (2010). Ultrastructural morphology of equine adipose-derived mesenchymal stem cells. Histol Histopathol, 25, 1277-1285.

18. Teti, G., Cavallo, C., Grigolo, B., et al. (2012). Ultrastructural analysis of human bone marrow mesenchymal stem cells during in vitro osteogenesis and chondrogenesis. Microsc Res Tech, 75, 596-604.

19. García-Prat, L., Martínez-Vicente, M., Muñoz-Cánoves, P. (2016). Autophagy: a decisive process for stemness. Oncotarget, 7, 12286-12288.

20. Sbrana, F.V., Cortini, M., Avnet, S., et al. (2016). The Role of Autophagy in the Maintenance of Stemness and Differentiation of Mesenchymal Stem Cells. Stem Cell Rev, 12, 621-633.

21. Iacono, E., Brunori, L., Pirrone, A., et al. (2012). Isolation, characterization and differentiation of mesenchymal stem cells from amniotic fluid, umbilical cord blood and Wharton's jelly in the horse. Reproduction, 143, 455-468.

22. Mattioli-Belmonte, M., Teti, G., Salvatore, V., et al. (2015). Stem cell origin differently affects bone tissue engineering strategies. Front Physiol, 6, 266.

23. Li, G., Zhang, X.A., Wang, H., et al. (2009). Comparative proteomic analysis of mesenchymal stem cells derived from human bone marrow, umbilical cord, and placenta: Implication in the migration. Proteomics, 9, 20-30.

24. Sart, S., Tsai, A.C., Li, Y., Ma, T. (2014). Three-dimensional aggregates of mesenchymal stem cells: cellular mechanism, biological properties, and applications. Tissue Eng Part B Rev, 20, 365-380.

25. Wang, W., Itaka, K., Ohba, S., et al. (2009). 3D spheroid culture system on micropatterned substrates for improved differentiation efficiency of multipotent mesenchymal stem cells. Biomaterials, 30, 2705-2715.

26. Suzuki, S., Muneta, T., Tsuji, K., et al. (2012). Properties and usefulness of aggregates of synovial mesenchymal stem cells as a source for cartilage regeneration. Arthritis Res Ther, 14, R136.

27. Mizuno, H., Hyakusoku, H. (2003). Mesengenic potential and future clinical perspective of human processed lipospirated cells. J Nippon Med Sch. 70, 300-306.

28. Janderova, L., McNeil, M., Murrell, A.N., Mynatt, R.L., Smith, S.R. (2003). Human mesenchymal stem cells as an in vitro model for human adipogenesis. Obes Res, 11, 65-74.

29. De Schauwer, C., Meyer, E., Van de Walle, G.R., Van Soom, A. (2011). Markers of stemness in equine mesenchymal stem cells: a plea for uniformity. Theriogenology, 75, 1431-1443.

Figure Legends

Fig. 1 Cell growth: doubling times of hWJMSCs (white) and eWJMSCs (black) over six passages of culture. * P<0.05

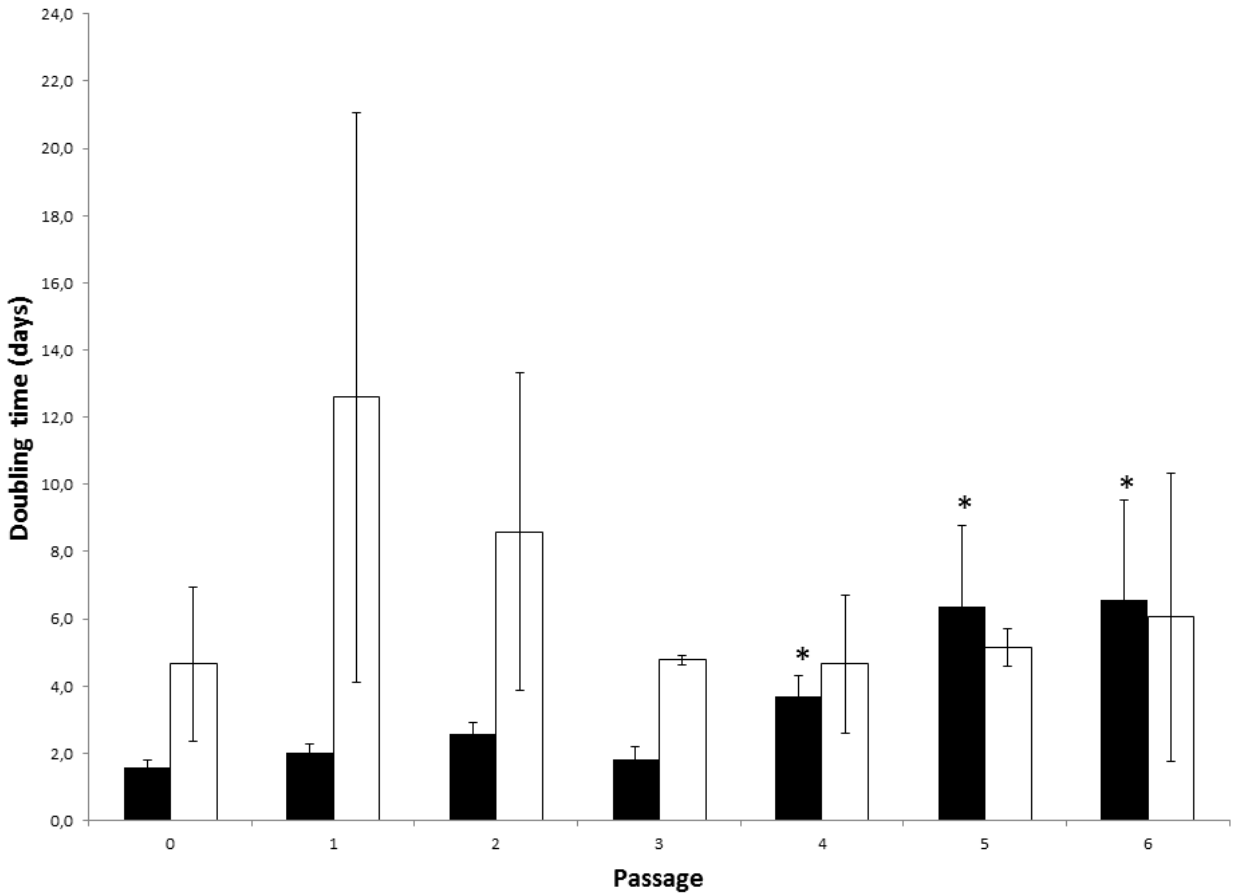

Fig. 2 Adhesion assay. (A) Volume reconstruction and visualization of an equine (on the left) and a human (on the right) WJMSCs spheroid obtained after 48 h of hanging drop culture, as assessed by ReVisp (scale in pixels). (B) Low ability of hWJMSCs to aggregate each other making micro- masses (scale bar 90µm)

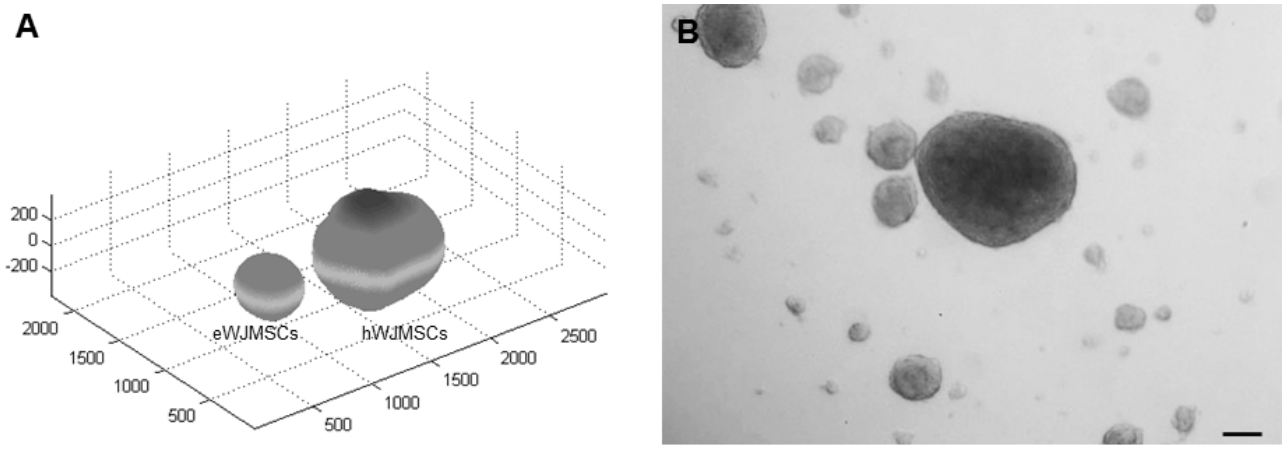

Fig. 3 Flow cytometry analysis of hWJMSCs for (A) CD105, (B) CD90, (C) CD73, (D) CD34, (E) CD19, (F) CD45, (G) HLA-DR and of eWJMSCs for (H) CD90 and (I) CD19. Representative single-variable histograms display negative control (white line) and the expression of cell surface antigens (grey)

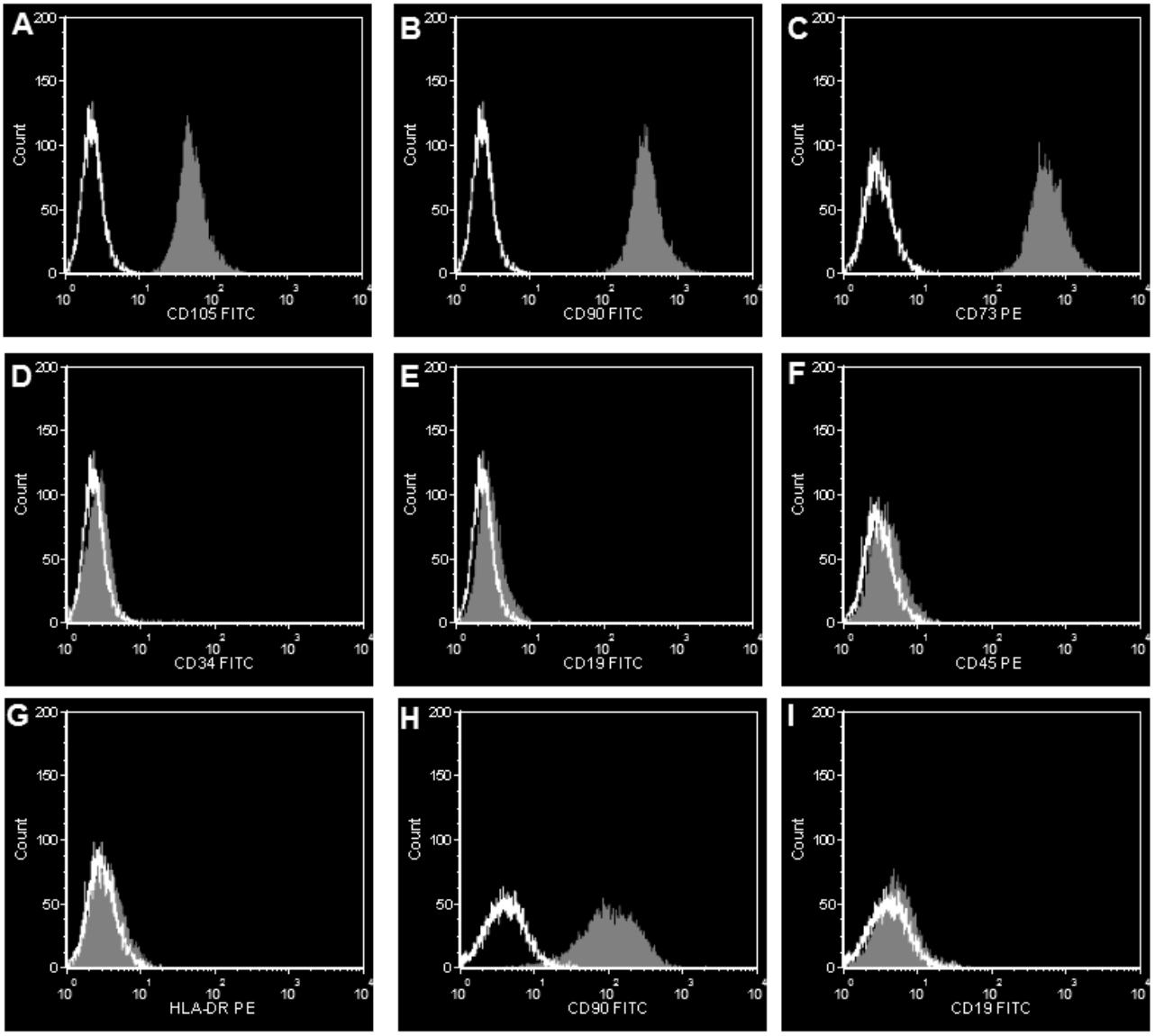

Fig. 4 TEM analysis of hWJMSCs. (A) cluster of cells showing a spindle shape morphology (scale bar 20µm); (B) detail of Golgi apparatus (black arrow) (scale bar 500nm) (C) detail of RER (black arrow) and mitochondria (m) (scale bar 1000nm); (D) detail of cytoplasm showing autophagy vesicles and autophagolysosomes (black arrowhead), RER (black arrow) (scale bar: 1000nm). Detail of a cell junction (insert; scale bar: 500nm). TEM analysis of eWJMSCs. (E) cluster of cells showing a spindle shape morphology (scale bar 10µm); (F) detail of Golgi (black arrows), mitochondria (m) and autophagy vesicle (black arrowhead) (scale bar 500 nm); (G) mitochondria (m), rough endoplasmic reticulum (black arrow), free ribosomes and autophagy vesicle (black arrowhead) in the cytoplasm of eWJMSCs (scale bar: 2000nm); (H)

detail of cytoplasm showing authopagy vesicles and autophagolysosomes (black arrowhead) (scale bar: 1000nm). Insert showing cellular junction (scale bar: 500nm)

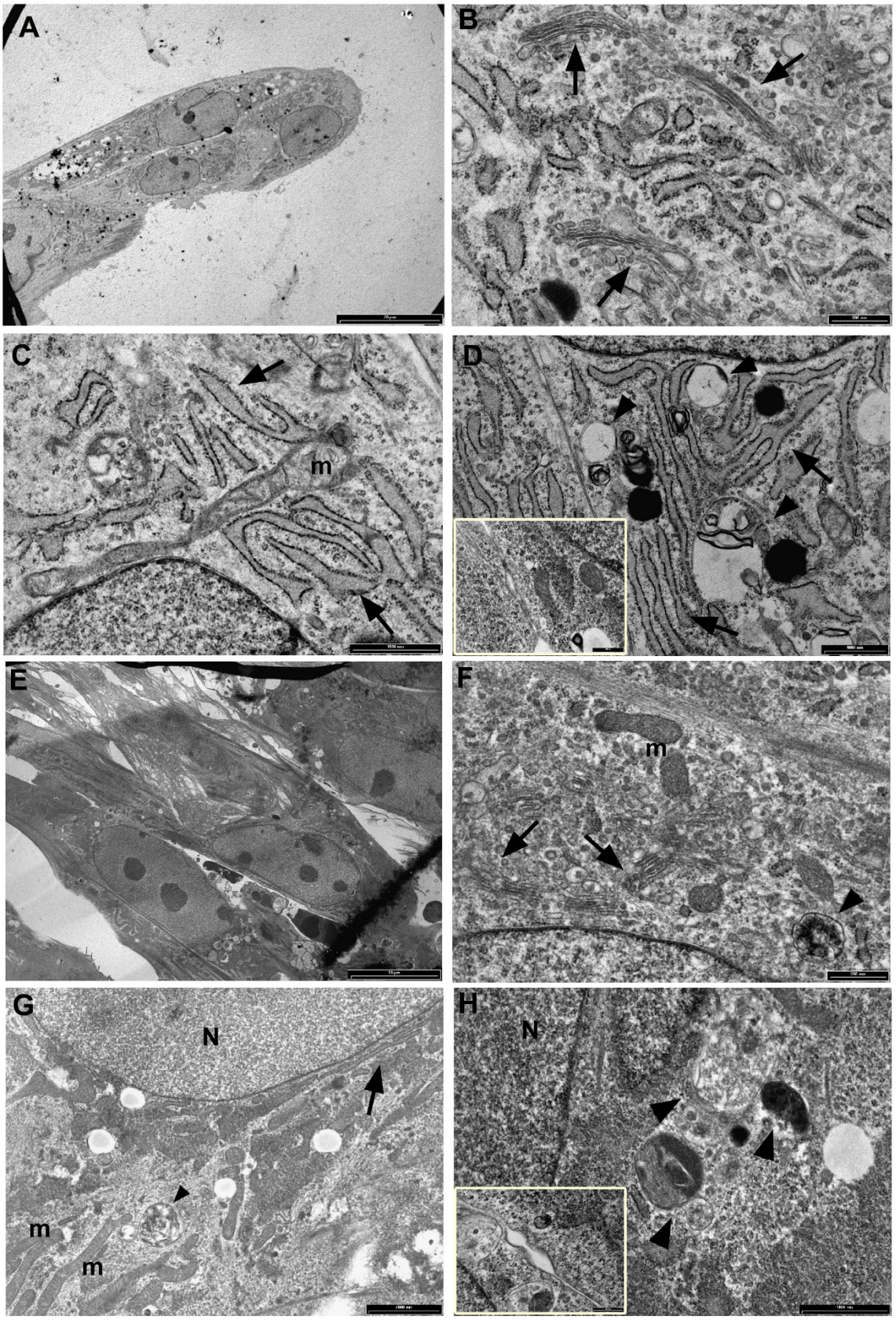

Fig. 5 Cell differentiation: (A) adipogenic differentiation of hWJMSCs after 10 days of induction (Oil Red O staining , scale bar 20 µm); (B) control samples consisting in hWJMSCs cultured with cell medium without any adipogenic factors (Oil Red O staining, scale bar 20 µm); (C) chondrogenic differentiation of hWJUMSCs after 21 days of induction (Alcian Blue staining, scale bar 20 µm); (D) control samples consisting in hWJMSCs cultured with cell medium without any chondrogenic factors (Alcian Blue staining, scale bar 20 µm); (E) osteogenic differentiation of hWJMSCs after 21 days of induction (Alizarin Red staining, scale bar 20 µm); (F) control samples consisting in hWJMSCs cultured with cell medium without any osteogenic factors (Alizarin Red staining, scale bar 20 µm)

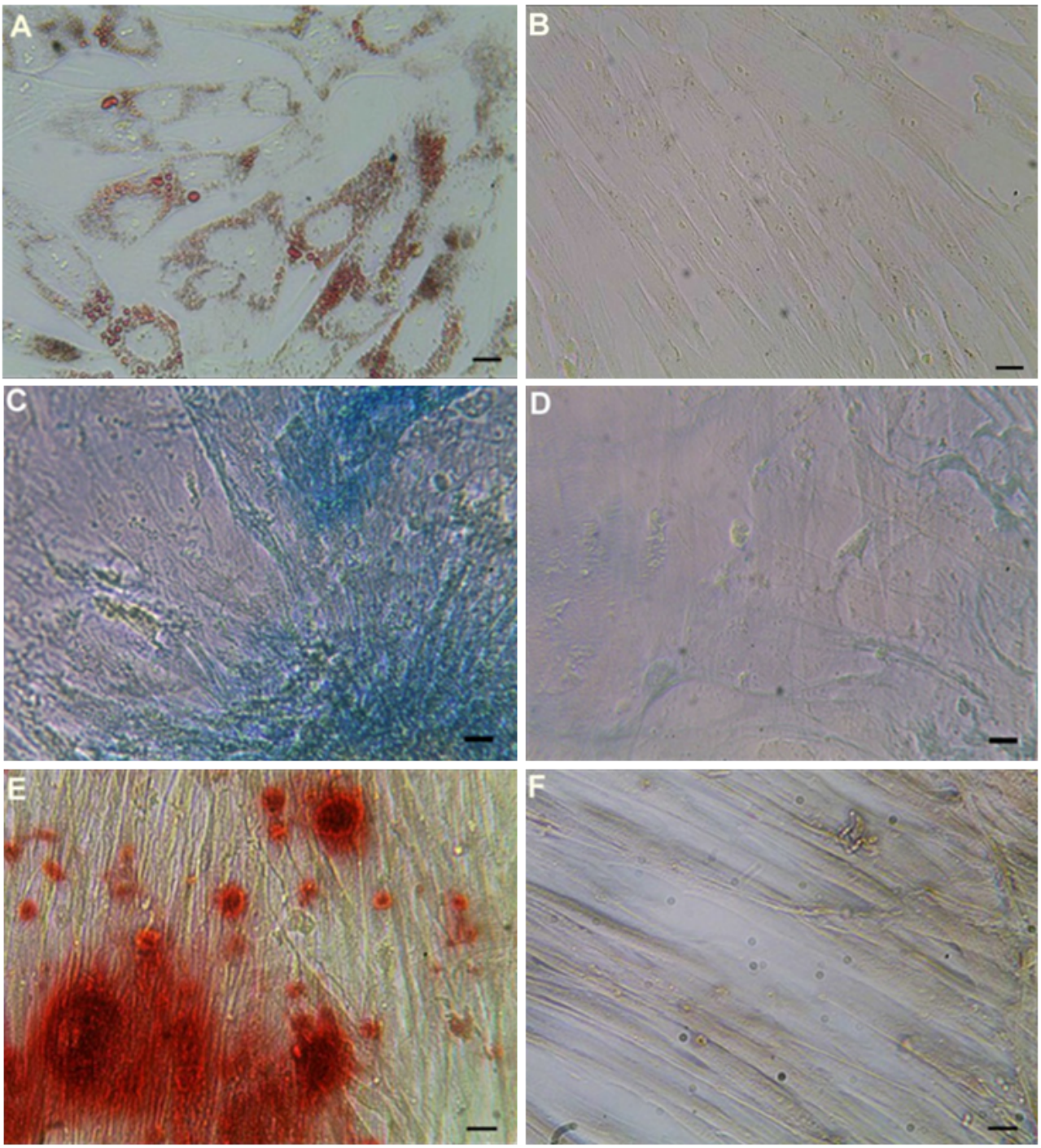

Fig. 6 Cell differentiation: (A) adipogenic differentiation of eWJMSCs after 10 days of induction (Oil Red O staining , scale bar 50 µm); (B) control samples consisting in eWJMSCs cultured with cell medium without any adipogenic factors (Oil Red O staining, scale bar 50 µm); (C) chondrogenic differentiation of eWJUMSCs after 21 days of induction (Alcian Blue staining, scale bar 50 µm); (D) control samples consisting in eWJMSCs cultured with cell medium without any chondrogenic factors (Alcian Blue staining, scale bar 50 µm); (E) osteogenic differentiation of eWJMSCs after 21 days of induction (Alizarin Red staining, scale bar 50 µm); (F) control samples consisting in eWJMSCs cultured with cell medium without any osteogenic factors (Alizarin Red staining, scale bar 50 µm)

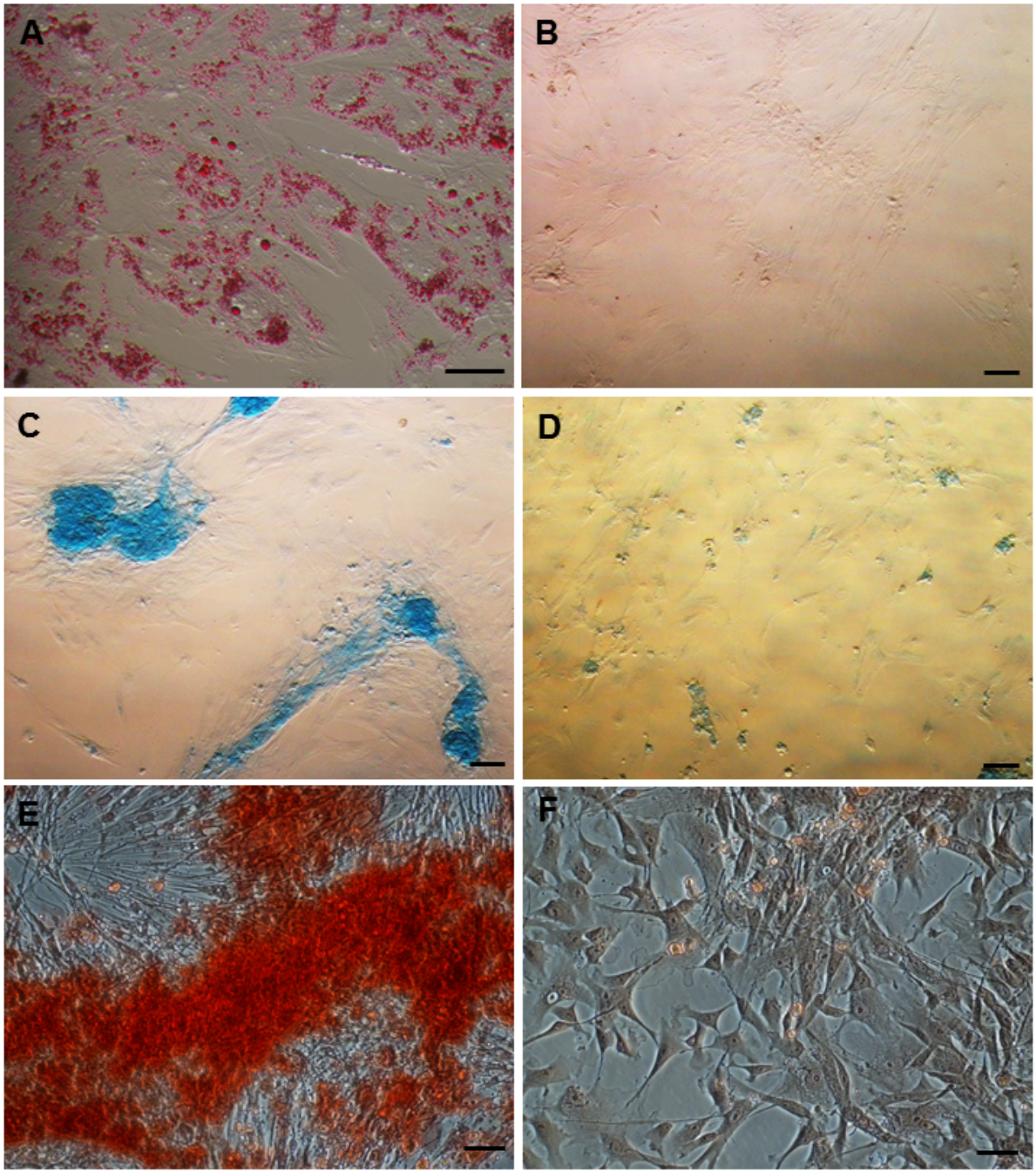

Tables

Table 1. Flow cytometry analysis of human and equine Wharton's jelly derived mesenchymal stem cells.

Group	CD105 (%)	CD90 (%)	CD73 (%)	CD34 (%)	CD19 (%)	CD45 (%)	HLA-DR (%)
hWJMSC	99.98	100.00	99.98	1.53	1.76	1.35	0.87
eWJMSC	n/a	92.57	n/a	n/a	n/a	n/a	n/a

hWJMSC: human Wharton's jelly derived mesenchymal stem cells; eWJMSC: equine Wharton's jelly derived mesenchymal stem cells; n/a: not applicable (no antibody cross-reactivity)